



Munich Personal RePEc Archive

# **Optimum cleaning schedule of photovoltaic systems based on levelised cost of energy and case study in central Mexico**

Rodrigo, Pedro M. and Gutiérrez, Sebastián and Micheli,  
Leonardo and Fernández, Eduardo F. and Almonacid,  
Florencia

20 September 2020

Online at <https://mpra.ub.uni-muenchen.de/104173/>  
MPRA Paper No. 104173, posted 31 Jan 2021 11:01 UTC

1 **Optimum cleaning schedule of photovoltaic systems based on levelised cost of energy**  
2 **and case study in central Mexico**

3 P.M. Rodrigo<sup>a,\*</sup>, S. Gutiérrez<sup>a</sup>, L. Micheli<sup>b</sup>, E.F. Fernández<sup>b</sup>, F.M. Almonacid<sup>b</sup>

4 <sup>a</sup> Universidad Panamericana. Facultad de Ingeniería. Josemaría Escrivá de Balaguer 101,  
5 Aguascalientes, Aguascalientes, 20290, México.

6 <sup>b</sup> Centre for Advanced Studies on Energy and Environment (CEAEMA), University of Jaén,  
7 Jaén, 23071, Spain.

8 \* Corresponding author

9 Tel.: 524499106200 ext. 7194

10 [prodrigo@up.edu.mx](mailto:prodrigo@up.edu.mx)

11 **Abstract**

12 In this paper, the soiling impact on photovoltaic systems in Aguascalientes, in central  
13 Mexico, an area where 1.4GWp of new photovoltaic capacity is being installed, is  
14 characterised experimentally. A soiling rate of -0.16 %/day in the dry season for optimally  
15 tilted crystalline silicon modules, and a stabilization of the soiling losses at 11.2% after 70  
16 days of exposure were observed. With this data, a first of its kind novel method for  
17 determining optimum cleaning schedules is proposed based on minimising the levelised cost  
18 of energy. The method has the advantages compared to other existing methods of considering  
19 the system investment cost in the determination of the optimum cleaning schedule. Also, it  
20 does not depend on economic revenue data, which is often subject to uncertainty. The results  
21 show that residential and commercial systems should be cleaned once per year in  
22 Aguascalientes. On the other hand, cleaning intervals from 12 to 31 days in the dry season  
23 were estimated for utility-scale systems, due to the dramatic decrease of cleaning costs per  
24 unit photovoltaic capacity. We also present a comparative analysis of the existing criteria for  
25 optimising cleaning schedules applied to the same case study. The different methods give  
26 similar cleaning intervals for utility-scale systems and, thus, the choice of a suitable method  
27 depends on the availability of information.

28 **Keywords:** cleaning schedule, crystalline silicon, levelised cost of energy, Mexico,  
29 photovoltaic, soiling.

## 30 Nomenclature

31	$a$	Fitting coefficient for modelling the soiling factor, day <sup>-1</sup>
32	$b$	Fitting coefficient for modelling the soiling factor, dimensionless
33	$C_0$	Photovoltaic system cost per kWp, USD/kWp
34	$C_{0\_ec}$	PV system cost financed through equity capital per kWp, USD/kWp
35	$C_{0\_loan}$	PV system cost financed through a loan per kWp, USD/kWp
36	$C_{clean}$	Cost of each cleaning operation per kWp, USD/kWp
37	$d$	Nominal discount rate, per unit
38	$d_{ec}$	Annual payback in the form of dividends, per unit
39	$F_{soil}$	Soiling factor, dimensionless
40	$G$	Plane-of-array global irradiance, W/m <sup>2</sup>
41	$i_l$	Annual loan interest, per unit
42	$I_{sc}$	Short-circuit current
43	$K_d$	Coefficient equal to $(1-r_d)/(1+d)$ , dimensionless
44	$K_p$	Coefficient equal to $(1+r_{OM})/(1+d)$ , dimensionless
45	$L_0, L_1, L_2$	Loss coefficients that characterise the inverter efficiency curve, 46 dimensionless
47	$L_{AC}$	Coefficient of losses in the AC-side, per unit
48	$LCC$	Life-cycle cost per kWp, USD/kWp
49	$LCOE$	Levelised cost of energy, USD/kWh
50	$L_{DC}$	Coefficient of losses in the DC-side, per unit
51	$N$	Number of years of the life cycle, years
52	$n_{clean}$	Number of cleaning operations per year, dimensionless
53	$N_d$	Tax life for depreciation, years
54	$N_l$	Years for the loan to be repaid, years
55	$p_{in}$	Input power to the inverter normalized to the inverter nominal power, 56 dimensionless
57	$p_l$	Fraction of the PV system cost financed through a loan, per unit
58	$PM_{10}$	Paticulate matter, particles with diameter lower than 10 $\mu\text{m}$ , $\mu\text{gr}/\text{m}^3$
59	$PM_{2.5}$	Paticulate matter, particles with diameter lower than 2.5 $\mu\text{m}$ , $\mu\text{gr}/\text{m}^3$
60	$p_{sys}$	Power generated by a 1 kWp photovoltaic system, kW/kWp
61	$PV_{AOM}$	Annual operation and maintenance cost per kWp, USD/kWp
62	$PW[DEP(N_d)]$	Present worth of the tax depreciation, USD/kWp
63	$PW[PV_{OM}(N)]$	Present worth of operation and maintenance cost per kWp, USD/kWp
64	$q$	Coefficient equal to $1/(1+d)$ , dimensionless
65	$r$	Normalization ratio of a measured module, dimensionless
66	$r_d$	Annual degradation rate of photovoltaic module efficiency, per unit
67	$r_{DCAC}$	DC-to-AC inverter sizing ratio, dimensionless
68	$r_{OM}$	Annual escalation rate of the operation and maintenance cost, per unit
69	$T$	Income tax rate, per unit
70	$t$	Time, days
71	$t_0$	Fitting coefficient for modelling the soiling factor, days

72	$T_{cell}$	Cell temperature, °C
73	$Y$	Annual energy yield, kWh/kWp
74		
75	<i>Greek symbols</i>	
76	$\gamma$	Temperature coefficient of maximum power, °C <sup>-1</sup>
77	$\Delta t$	Time step for the simulations, h
78	$\eta_{inv}$	Inverter efficiency, per unit
79		
80	<i>Abbreviations</i>	
81	AC	Alternating Current
82	CENACE	Centro Nacional de Control de Energía
83	CGSMN	Coordinación General del Servicio Meteorológico Nacional
84	CONAGUA	Comisión Nacional del Agua
85	DC	Direct Current
86	IEC	International Electrotechnical Commission
87	INECC	Instituto Nacional de Ecología y Cambio Climático
88	MBE	Mean Bias Error
89	PV	Photovoltaic
90	RMSE	Root Mean Square Error
91	WACC	Weighted Average Cost of Capital
92		

## 93 **1. Introduction**

94 The natural deposition of dust, particles and, dirt on the photovoltaic (PV) modules, named  
95 soiling, can affect significantly the energy generation of PV systems. Soiling accumulates  
96 during the dry periods between cleaning events, and can be naturally removed by rain and  
97 other natural events, or artificially removed by cleaning the PV modules. Determining a good  
98 cleaning strategy is essential for improving the profitability of a PV system, where a careful  
99 balance between the cost of cleaning operations and the benefits obtained in the form of  
100 increasing energy yield (and increasing revenues) must be considered.

101 The scientific community is paying great attention to the mechanisms and impact of soiling  
102 in solar energy systems because of the influence in energy production and economics of solar  
103 plants worldwide (Costa et al., 2018, 2016). However, there are not many findings dealing  
104 with optimisation of cleaning schedules, a critical topic especially regarding utility-scale PV  
105 plants, where small drops in the energy yield cause impressive economic losses and large  
106 operation and maintenance teams are involved. Some authors have characterised the soiling  
107 impact at specific sites and have given recommendations for cleaning in a qualitative way.

108 In (Kalogirou et al., 2013), three PV technologies (mono-crystalline, poly-crystalline and  
109 amorphous silicon) were experimentally analysed in Cyprus considering the episodes of dust  
110 storms from North Africa. Authors recommended cleaning the systems every 2-3 weeks in  
111 the dry season. In (Fuentealba et al., 2015), the energy yield of two PV technologies (poly-  
112 crystalline and, amorphous/microcrystalline silicon) was monitored during 1.5 years at the  
113 Atacama Desert and, based on the experimental data, authors recommended cleaning  
114 schedules by differentiating between summer and winter seasons and, between both  
115 technologies. In (Jiang et al., 2016), authors developed a physical model that characterises  
116 the rate of particle deposition in desert regions. The cleaning operations were then  
117 recommended when the efficiency loss due to soiling reaches 5% compared to the clean  
118 efficiency. In (Fathi et al., 2017), authors evaluated the “soiling threshold” for two PV  
119 technologies (mono-crystalline silicon and, CdTe) in Algeria. This minimum soiling loss  
120 makes profitable a two-cleanings per year schedule, and corresponds to 7.3% for mono-  
121 crystalline and, 6.8% for CdTe. In (Conceição et al., 2019), a model intended for calculating  
122 the effective irradiance under soiling as a function of the PV module tilt angle at the Alentejo  
123 region, Portugal, was developed. By comparing the effective irradiance in soiled and clean  
124 scenarios, the period of the year in which it would be desirable to perform cleaning operations  
125 can be determined, but not the time interval for cleaning schedule. These contributions have  
126 as a common feature that the cleaning operations are recommended based on the criterion of  
127 the experts.

128 Other authors have implemented criteria that are more systematic. In (Tanesab et al., 2018),  
129 the cleaning schedule of grid-connected and stand-alone PV systems in Australia and  
130 Indonesia was determined by matching the annual revenue loss due to soiling to the annual  
131 cleaning cost. This criterion was also used in (Sulaiman et al., 2018) giving a 2.5 months  
132 interval between cleaning operations in Malaysia. A similar approach was applied in  
133 Santiago, Chile, by monitoring the performance ratio of mono-crystalline, poly-crystalline  
134 and, amorphous silicon during two years, and defining a critical interval of 45 days between  
135 cleaning operations for the three technologies (Urrejola et al., 2016). A different criterion,  
136 based on formulating an optimisation problem that maximizes the difference between annual  
137 revenues and annual cleaning costs, was used in (Besson et al., 2017), also applied to the  
138 soiling characterisation of three PV technologies during 2.5 years in Santiago, Chile. This

139 methodology was modified in (Luque et al., 2018) for analysing bifacial modules and  
140 differentiating the cleaning schedules for the front surface and the back surface of the  
141 modules. Another approach in Saudi Arabia considered the problem of minimising the  
142 function  $(V_L + C_C)/V_S$ , where  $V_L$  is the annual revenue loss due to soiling,  $C_C$  is the annual  
143 cleaning cost and,  $V_S$  is the annual revenue (Jones et al., 2016). All of these criteria use an  
144 objective function in a particular year of operation. To our knowledge, there is only one  
145 contribution that has proposed an objective function extended over the whole life cycle of  
146 the PV system, i.e. maximising the Net Present Value (You et al., 2018). In this study, seven  
147 cities worldwide were analysed based on one year of experimental data.

148 In this paper, we propose a novel method for optimising the cleaning schedule based on  
149 minimising the levelised cost of energy (*LCOE*). Similarly to the approach in (You et al.,  
150 2018), and differentiating from the other reviewed approaches, we consider an objective  
151 function extended over the whole life cycle of the PV system, which should give more  
152 reliable results. By using this method, the influence of the system investment cost, which can  
153 vary significantly as a function of the system size, on the optimum cleaning schedule is  
154 analysed for the first time. One of the advantages of this method compared to the rest of  
155 reviewed methods is that it does not require economic revenue data, which is often subject  
156 to uncertainty. In addition, in the last part of the study, we present a comparative analysis of  
157 the different existing criteria for optimising cleaning schedules applied to the same case  
158 study. This is the first time this kind of analysis is done and it sheds light on the choice of the  
159 existing alternatives.

160 The method is applied to the semi-desert climatic and soiling conditions of Aguascalientes,  
161 central Mexico. Aguascalientes State, in spite of its small size (5616 km<sup>2</sup>), is highlighting as  
162 one of the most important regions in Mexico for PV system facilities. This is because it  
163 combines a high solar resource (2125 kWh/m<sup>2</sup>/year global horizontal irradiation according  
164 to the data used in this study, see section 2.1) with temperatures warmer than the Northern  
165 deserts of Mexico, and lower soiling impact. The PV projects that were awarded in the last  
166 three long-term auctions derived from the energetic reform in Mexico corresponding to  
167 Aguascalientes State are presented in Table 1 (Centro nacional de Control de Energía  
168 (CENACE), 2018). As can be seen, a total of 1429 MWp PV power has been or is going to

169 be installed imminently in this State thanks to its high solar potential. The results presented  
170 in this paper are supported by the experimental measurements of soiling factors registered in  
171 Aguascalientes. To the best of our knowledge, there is only one paper analysing the soiling  
172 impact in Mexico, and it corresponds to the Northern Sonora’s desert (Cabanillas and  
173 Munguía, 2011). In that paper, the soiling losses of three PV technologies (mono-, poly- and,  
174 amorphous silicon) were characterised, but no conclusions on the optimum cleaning schedule  
175 were extracted. The present paper will provide a robust tool to characterize the soiling loss  
176 at a site and to identify the most convenient cleaning schedule, in order to maximize the  
177 energy yield and the profitability of PV systems.

178 Table 1. PV projects awarded in the last three long-term auctions in Mexico corresponding  
179 to Aguascalientes State (Centro nacional de Control de Energía (CENACE), 2018).

Name of the project	Company	Country	Peak power (MWp)
Solem I - Solem II	Alten	Spain - Canada - Mexico	350
Pachamama	Neoen	France	300
Tepezalá II Solar	Consortio SMX	Mexico - USA	300
Trompezón	Engie	France	126
Las Viborillas	Jinkosolar Investment	China	100
Horus AG	Canadian Solar	Canada - Mexico	95
Aguascalientes Potencia 1	Recurrent Energy Mexico Development	Canada - Mexico	63
Aguascalientes Sur 1	OPDE	Spain	59
San Bartolo	Infraestructura Energética del Norte	Mexico	34.9
Parque Solar Bicentenario	Autoabastecimiento Renovable	Mexico	0.79

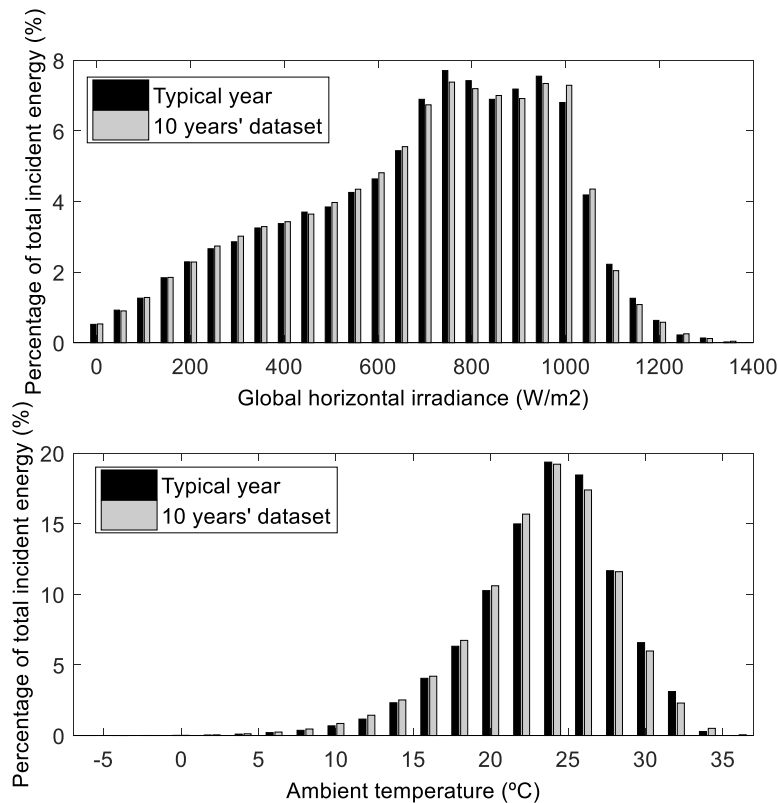
180

## 181 **2. Materials and methods**

### 182 **2.1. Atmospheric data**

183 Typical data of global horizontal irradiance, ambient temperature, rainfall and, particulate  
184 matter of Aguascalientes city (21.9°N, -102.3°E) have been collected for carrying out this  
185 study. The global horizontal irradiance and ambient temperature data were supplied by the  
186 Coordinación General del Servicio Meteorológico Nacional (CGSMN) of the Comisión  
187 Nacional del Agua (CONAGUA). It is a dataset that covers 10 years of measurements (from

188 December 2005 to April 2015) at 10-minute intervals taken at an atmospheric station near  
189 the center of the city. This dataset has been processed to get the typical year of irradiance and  
190 temperature. For each month (January, February, etc.), we have searched the month in the  
191 dataset that better matches the average monthly global horizontal irradiation. For instance,  
192 considering January, January 2009 had  $4.62 \text{ kWh/m}^2/\text{day}$ , which is close to the average  $4.54$   
193  $\text{kWh/m}^2/\text{day}$  obtained for all the January months in the dataset. These real months from  
194 different years are linked to get the typical meteorological year of global irradiance and  
195 temperature (Rodrigo et al., 2016). In addition, the histograms of irradiance and temperature  
196 have been analysed to guarantee that the generated typical year has a similar distribution than  
197 the 10 years' dataset. As an example of these histograms, the annual distribution of irradiance  
198 and temperature is shown in Fig. 1, where an acceptable matching between the typical year  
199 and the 10 years' dataset can be observed. As a conclusion, we assessed that the generated  
200 typical year represents adequately the average climate of the location.



201

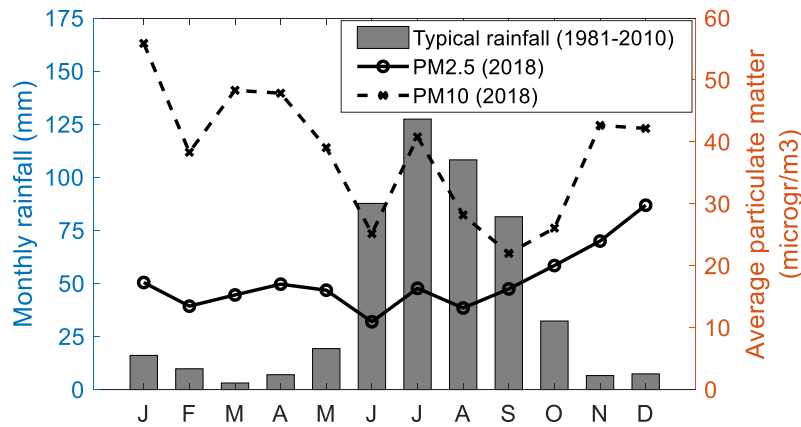


202 Fig. 1. Comparison between the annual histograms of global horizontal irradiance (top) and  
203 ambient temperature (bottom) corresponding to the generated typical year and the 10 years'  
204 dataset in Aguascalientes.

205 In this study, south-oriented 20° tilted PV systems are considered, which is the typical  
206 configuration of mounting structures in the region and represents optimum tilt and orientation  
207 to maximise annual energy harvesting for fixed structure systems in Aguascalientes. The  
208 three components of solar radiation (direct, diffuse and albedo) on the plane of the PV  
209 generator have been modelled. The Iqbal's correlation to compute the diffuse fraction (Iqbal,  
210 1983), the Hay's anisotropic sky diffuse model (Hay, 1979) and, an isotropic model with  
211 constant albedo coefficient of 20% are used for this purpose, according to previously  
212 published contributions (Rodrigo, 2017; Rodrigo et al., 2016; Sánchez-Carbajal and Rodrigo,  
213 2019). In addition, the cell temperature of the PV modules is calculated from ambient  
214 temperature and plane-of-array global irradiance based on the Nominal Operating Cell  
215 Temperature method (International Electrotechnical Commission (IEC), 2011).

216 The monthly average rainfall in the 1981-2010 period has been retrieved from (Servicio  
217 Meteorológico Nacional, 2019) and is shown in Fig. 2. It can be seen that the typical  
218 meteorological year in Aguascalientes can be divided into two seasons: the dry season,  
219 covering a period of eight months from October to May and, the wet season, covering a  
220 period of four months from June to September. In the dry season, the rainfall events are very  
221 scarce in this region, with a mean monthly rainfall of 12.7 mm. In the wet season, there are  
222 frequent storms, typically every day, and the mean monthly rainfall is 101.2 mm. In the wet  
223 period, the 80% of the accumulated rainfall occurs. The monthly average particulate matter  
224 ( $PM_{2.5}$  and  $PM_{10}$ ) calculated as the average of the daily measurements is also represented  
225 in Fig. 2 for the year 2018, taken from (Instituto Nacional de Ecología y Cambio Climático  
226 (INECC), 2019). Regarding  $PM_{2.5}$ , the behaviour in 2018 was quite stable over the whole  
227 year, with monthly average values between 10 and 29  $\mu\text{gr}/\text{m}^3$ , and no important seasonal  
228 variations. Regarding  $PM_{10}$ , it can be differentiated two different levels of particulate matter  
229 in 2018: one that covers approximately the dry season (values between 39 and 56  $\mu\text{gr}/\text{m}^3$ ,  
230 except for the anomalous October, with 26  $\mu\text{gr}/\text{m}^3$ ) and, another that covers approximately  
231 the wet season (values between 22 and 28  $\mu\text{gr}/\text{m}^3$ , except for the anomalous July, with 41

232  $\mu\text{gr}/\text{m}^3$ ). By analysing these values of 2018, it can be said that the  $PM_{2.5}$  behaviour seems to  
233 be stable over the year, while the  $PM_{10}$  behaviour could be divided into the dry season (with  
234 higher values) and the wet season (with lower values). It can be highlighted that neither  
235  $PM_{2.5}$  nor  $PM_{10}$  show appreciable seasonality effects in the dry season, which is the focus  
236 of the soiling analysis in this paper.



237

238 Fig. 2. Monthly average rainfall (1981-2010) and average particulate matter (2018) in  
239 Aguascalientes (Instituto Nacional de Ecología y Cambio Climático (INECC), 2019;  
240 Servicio Meteorológico Nacional, 2019).

## 241 2.2. Experimental set-up and soiling characterisation

242 An experimental set-up was installed at the research facilities of the Engineering Faculty of  
243 Panamericana University in Aguascalientes. The set-up consisted in three 60-cells poly-  
244 crystalline PV modules, model Risen RSM60-6-260P, mounted on a south-oriented  $20^\circ$  tilted  
245 structure (Fig. 3). The characteristics of the modules at Standard Test Conditions are shown  
246 in Table 2. The aim of the set-up is to measure the soiling factor ( $F_{soil}$ ) of two modules, which  
247 are naturally soiled, taking as reference the third module, which is cleaned each day of  
248 measurement. Before beginning the soiling characterisation, it was necessary to check that  
249 the three modules have very similar electrical response. For this purpose, the three modules  
250 were perfectly cleaned, and exposed to natural sunlight during a clear day. The simultaneous  
251 measurement of the three short-circuit currents at 15-minute intervals from 10:00 a.m. to 4:00  
252 p.m. are shown in Fig. 4. The numerical values of Mean Bias Error (MBE) and Root Mean  
253 Square Error (RMSE) of the modules A and B (those that will be exposed to natural soiling)

254 with reference to the third module, which will be cleaned during the experimental campaign,  
255 are shown in Table 3. The obtained errors are small enough for soiling measurements. The  
256 normalization ratio of each module ( $r$ ) is also shown in the table, understood as the average  
257 ratio of short-circuit current of the module to the short-circuit current of the reference module.



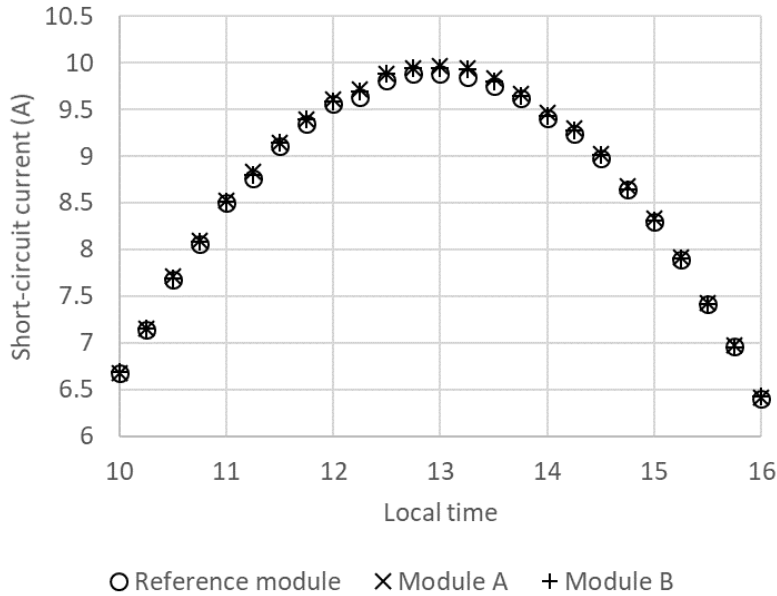
258

259 Fig. 3. Photo of the experimental set-up at the facilities of Panamericana University,  
260 Aguascalientes campus.

261 Table 2. Characteristics of the analysed PV modules at Standard Test Conditions.

<b>Parameter</b>	<b>Value</b>
Maximum power	260 W <sub>p</sub>
Power tolerance	0-4.99 W
Maximum power point voltage	30.6 V
Maximum power point current	8.50 A
Open-circuit voltage	37.8 V
Short-circuit current	9.04 A
Module efficiency	15.9 %
Nominal operating cell temperature	45±2 °C
Temperature coefficient of maximum power	-0.39 %/°C

262



263

264 Fig. 4. Measurements of the short-circuit currents of the three analysed PV modules after  
 265 cleaning over a clear day from 10:00 a.m. to 4:00 p.m. The reference module is the one that  
 266 will be kept clean over the soiling characterisation.

267 Table 3. Mean Bias Error (MBE) and Root Mean Square Error (RMSE), calculated from  
 268 short-circuit current measurements of the modules A and B compared to the reference  
 269 module. The normalization ratio of each module is also shown.

PV module	MBE (%)	RMSE (%)	Normalization ratio ( <i>r</i> )
A	0.49	0.56	1.004923
B	0.32	0.40	1.003153

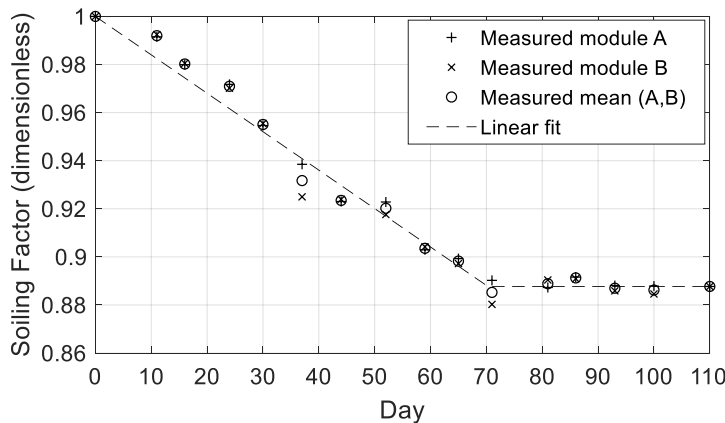
270

271 An experimental campaign of 110 days was carried out in the dry season of 2019. During  
 272 this campaign, modules A and B were not cleaned and, thus, were exposed to natural soiling.  
 273 The reference module was cleaned periodically in intervals from 5 to 10 days. Each day the  
 274 reference module was cleaned, a set of six measurements of the short-circuit currents was  
 275 performed at 15-minute intervals around noon. As the short-circuit currents were measured  
 276 around noon, angle-of-incidence, spectral and, low irradiance effects, which could distort the  
 277 measurements, were avoided. Measurements under cloudy conditions (global horizontal  
 278 irradiance < 500 W/m<sup>2</sup>) were also removed to avoid low irradiance uncertainties. The soiling  
 279 factor of module “*i*” ( $F_{soil,i}$ ) for each measurement is defined in this study as the ratio of the  
 280 short-circuit current of the “*i*” soiled module ( $I_{sc,i,soil}$ ) to the short-circuit current of the

281 reference clean module ( $I_{sc,ref, clean}$ ), divided by the normalization ratio of the “ $i$ ” soiled module  
282 ( $r_i$ ):

$$283 \quad F_{soil,i} = \frac{I_{sc,i,soil} / I_{sc,ref, clean}}{r_i} \quad (1)$$

284 The soiling factor is equivalent to the soiling ratio used by other authors (International  
285 Electrotechnical Commission, 2017). The soiling losses can be extracted as  $1 - F_{soil,i}$ , and are  
286 here expressed as percent. The six measurements were averaged each cleaning day to get the  
287  $F_{soil}$  for that day. Thus,  $F_{soil}$  of modules A and B with reference to the clean module were  
288 obtained every 5-10 days during the experimental campaign. The behaviour of  $F_{soil}$  of  
289 modules A and B over this experiment is shown in Fig. 5. (Gostein et al., 2013) showed that  
290 the  $F_{soil}$  measured from short-circuit currents is a very good approach to correct the maximum  
291 power of soiled PV modules, in conditions of uniform soiling and loss level below 11%. For  
292 heavier soiling, nonuniformity of illumination and soil accumulating near the module corners  
293 can cause current matching in strings and hot temperatures in some cells, which would  
294 invalidate the approach based on the short-circuit current measurement (Gostein et al., 2014).  
295 In our experiment, maximum soiling losses of about 11%, corresponding to a soiling factor  
296 of 0.89, were registered, and visual inspection of the soiled modules for checking the uniform  
297 deposition was done, so that the approach based on short-circuit current measurements can  
298 be considered adequate.



299

300 Fig. 5. Measurement of the soiling factor of modules A and B during the experimental  
301 campaign, and linear fit of the data for modelling purposes.

302 The experimental data in Fig. 5 allowed the natural soiling of optimally tilted crystalline PV  
303 modules in the dry season of Aguascalientes to be characterised. As can be seen, the  $F_{soil}$   
304 follows an approximately linear descendent behaviour until a threshold value, in which  
305 soiling losses stabilize. This behaviour is similar to that observed in other published studies,  
306 for instance in (Kalogirou et al., 2013), where the soiling losses stabilized after nine weeks  
307 of exposure in the summer season of Cyprus. Taking into account the experimental data, the  
308  $F_{soil}$  after a cleaning operation in the dry season can be modelled as a function of time ( $t$  in  
309 days) as:

$$310 \quad F_{soil}(t) = \begin{cases} 1 - a \cdot t, & t \leq t_0 \\ b, & t > t_0 \end{cases} \quad (2)$$

311 With fitted values of  $a = 0.001598$  ( $R^2 = 0.977$ ),  $b = 0.8877$  and,  $t_0 = 70.3$  (Fig. 5). This means  
312 that the natural soiling in the dry season follows a soiling rate (here labelled as  $a$ ) of -0.16  
313 %/day until the 70<sup>th</sup> day after cleaning, in which soiling losses stabilize at 11.2%.

314 In this work, the soiling factor profile is built according to the Fixed Rate Precipitation model  
315 (Kimber et al., 2007). This is the first, and still one of the most common, soiling extraction  
316 model and is based on the assumption that the soiling factor profile at a site can be determined  
317 by alternating soiling deposition periods (that follow Eq. (2)) and cleaning events, that raise  
318 the soiling factor to 1. In this work, only rainfall events are found to have a cleaning effect  
319 on the photovoltaic modules. Therefore, the soiling profile in this work is built based on the  
320 previously shown wet and dry periods. No soiling accumulation occurs during the wet season,  
321 because of the daily frequency of rainfalls. For this reason, the soiling factor is assumed to  
322 be 1 during the wet months. On the other hand, there were no rainfall events during the 110  
323 day experimental campaign, which is the typical climatic behaviour in the dry season of  
324 Aguascalientes. It can be also highlighted that the soiling behaviour was very similar for the  
325 modules A and B, as can be seen in Fig. 5, which gives reliability to the soiling  
326 characterisation. In this study, the  $F_{soil}$  is assumed to propagate according to Eq. (2) after a  
327 cleaning operation in the dry season. This means that we assume the soiling rate to be  
328 constant during the dry season, in accordance also with the original model proposed by  
329 (Kimber et al., 2007). The seasonal variability of soiling rates is currently object of intense  
330 research (Micheli et al., 2019, 2017). However, in the specific climate of Aguascalientes, the

331 particulate matter levels in the dry season are quite stable (Fig. 2), so that appreciable changes  
332 in the soiling deposition rates are not expected (Coello and Boyle, 2019).

### 333 **2.3. Energy yield model**

334 The power generated by a PV system of 1 kWp capacity (in kW/kWp) can be expressed as:

$$335 \quad p_{sys} = \frac{G}{1000 \text{ W/m}^2} \cdot F_{soil} \cdot [1 + \gamma \cdot (T_{cell} - 25^\circ \text{C})] \cdot (1 - L_{DC}) \cdot \eta_{inv} \cdot (1 - L_{AC}) \quad (3)$$

336 Where  $G$  is the plane-of-array global irradiance ( $\text{W/m}^2$ ),  $F_{soil}$  is the soiling factor for the day  
337 considered (per unit),  $\gamma$  is the temperature coefficient of maximum power of the PV modules  
338 ( $^\circ\text{C}^{-1}$ ),  $T_{cell}$  is the cell temperature ( $^\circ\text{C}$ ),  $L_{DC}$  is the coefficient representing losses in the DC-  
339 side in per unit (angular, spectral, low irradiance, shading, electrical mismatch and, DC wires  
340 heating),  $\eta_{inv}$  is the inverter efficiency (per unit) and,  $L_{AC}$  is the coefficient representing losses  
341 in the AC-side in per unit (AC wires heating and, power transformer if present). In this study,  
342 soiling, temperature and, inverter losses are calculated in detail, while the rest of DC and AC  
343 losses are represented by typical average annual coefficients, i.e.  $L_{DC}$  of 7.5% and,  $L_{AC}$  of  
344 1.5% (Rus-Casas et al., 2014).

345 The inverter efficiency is calculated from the DC input power to the inverter normalized to  
346 the inverter nominal power ( $p_{in}$ ), which can be expressed as:

$$347 \quad p_{in} = r_{DCAC} \cdot \frac{G}{1000 \text{ W/m}^2} \cdot F_{soil} \cdot [1 + \gamma \cdot (T_{cell} - 25^\circ \text{C})] \cdot (1 - L_{DC}) \quad (4)$$

348 Where  $r_{DCAC}$  is the DC-to-AC inverter-sizing ratio, or ratio of PV array peak power to inverter  
349 nominal power.  $r_{DCAC}$  is set in this study to 1.2 according to optimal values found for  
350 crystalline silicon modules in Aguascalientes (Rodrigo et al., 2016). The inverter efficiency  
351 can then be calculated by:

$$352 \quad \eta_{inv} = \min \left\{ 1 - \left( L_0 + L_1 p_{in} + L_2 p_{in}^2 \right) / p_{in}, 1 / p_{in} \right\} \quad (5)$$

353 Where  $L_0=0.0048$ ,  $L_1=0.0159$  and,  $L_2=0.0144$  are the inverter loss coefficients representing  
354 typical medium efficiency inverters taken from (Pérez-Higueras et al., 2018). The first term  
355 in Eq. (5) corresponds to normal operating conditions, while the second term corresponds to

356 the conditions in which the inverter limits the output power to its nominal power in periods  
357 of high irradiance.

358  $F_{soil}$  is assumed to propagate according to Eq. (2) after each cleaning operation in the dry  
359 season, while it is set to one in the wet season, as no soiling deposits because of the daily rain  
360 events. Therefore, the pessimistic approach that there are not rainfall events in the dry season,  
361 and the optimistic approach that the frequent rainfall events in the wet season keep the  
362 modules perfectly clean, are used in this study to estimate the energy yield. Also, when a  
363 cleaning operation is performed in the dry season,  $F_{soil}$  is reinitialized to one and a positive  
364 offset is transmitted until the following rainfall. These assumptions allow the energy yield  
365 calculation to be simplified and are expected to be valid for the climate of Aguascalientes in  
366 a long-term life cycle analysis.

367 The annual energy yield in kWh/kWp/year ( $Y$ ) is obtained as:

$$368 \quad Y = \sum_{year} P_{sys,i} \cdot \Delta t \quad (6)$$

369 Where  $\Delta t$  is the time step for the simulation (1/6 hr in this study).

#### 370 **2.4. Levelised cost of energy model**

371 The methodology for calculating the  $LCOE$  is similar to that proposed in (Talavera et al.,  
372 2019). The general formulation of the  $LCOE$  in this study is:

$$373 \quad LCOE = \frac{LCC}{Y \cdot \frac{K_d \cdot (1 - K_d^N)}{1 - K_d}} \quad (7)$$

$$374 \quad K_d = (1 - r_d) / (1 + d) \quad (8)$$

375 Where  $LCC$  is the life-cycle cost per kWp-installed capacity,  $N$  is the number of years of the  
376 life cycle,  $r_d$  is the annual degradation rate of PV module efficiency, and  $d$  is the nominal  
377 discount rate. The  $LCC$  can be broken down as:

$$378 \quad LCC = C_0 + PW[PV_{OM}(N)] - PW[DEP(N_d)] \cdot T \quad (9)$$



379 Where  $C_0$  is the system cost per kWp,  $PW[PV_{OM}(N)]$  is the present worth of operation and  
380 maintenance cost per kWp,  $PW[DEP(N_d)]$  is the present worth of the tax depreciation, and  $T$   
381 is the income tax rate.

382 Concerning the operation and maintenance cost of the life cycle of the system,  $PW[PV_{OM}(N)]$   
383 can be written as:

$$384 \quad PW[PV_{OM}(N)] = PV_{AOM} \cdot (1-T) \cdot \frac{K_p \cdot (1-K_p^N)}{1-K_p} \quad (10)$$

$$385 \quad K_p = (1+r_{OM})/(1+d) \quad (11)$$

386 Where  $PV_{AOM}$  is the annual operation and maintenance cost per kWp, and  $r_{OM}$  is the annual  
387 escalation rate of the operation and maintenance cost.  $r_{OM}$  takes the value of the average  
388 inflation rate in this study.  $PV_{AOM}$  is the product of the number of cleaning operations per  
389 year ( $n_{clean}$ ) by the cost of each cleaning operation per kWp-installed capacity ( $C_{clean}$ ):

$$390 \quad PV_{AOM} = n_{clean} \cdot C_{clean} \quad (12)$$

391 The tax depreciation is calculated as linear over the time period:

$$392 \quad PW[DEP(N_d)] = \frac{C_0}{N_d} \cdot \frac{q \cdot (1-q^{N_d})}{1-q} \quad (13)$$

$$393 \quad q = 1/(1+d) \quad (14)$$

394 Where  $N_d$  is the tax life for depreciation in years.

395 The share of debt financing and equity financing can be included in the analysis explicitly  
396 through the weighted average cost of capital (WACC) over the discounting factor (nominal  
397 discount rate).  $C_0$  is assumed to be financed through debt -a loan- ( $C_{0\_loan}$ ) and equity capital  
398 ( $C_{0\_ec}$ ) so that can be written as:

$$399 \quad C_0 = C_{0\_loan} + C_{0\_ec} \quad (15)$$

400 The  $C_{0\_loan}$  and  $C_{0\_ec}$  can then be evaluated as:

$$401 \quad C_{0\_loan} = (p_l \cdot C_0) \cdot \frac{i_l \cdot (1-T)}{1 - [1 + i_l \cdot (1-T)]^{-N_l}} \cdot \frac{q \cdot (1 - q^{N_l})}{1 - q} \quad (16)$$

$$402 \quad C_{0\_ec} = d_{ec} \cdot [(1 - p_l) \cdot C_0] \cdot \frac{q \cdot (1 - q^N)}{1 - q} + [(1 - p_l) \cdot C_0] \cdot q^N \quad (17)$$

403 Where  $p_l$  is the fraction of system cost financed through a loan,  $i_l$  is the annual loan interest,  
404  $N_l$  are the years for the loan to be repaid, and  $d_{ec}$  is the annual payback in the form of  
405 dividends.

406 It is worth mentioning that the left-hand side of Eq. (15) only equals its right-hand side if the  
407 selected value of  $d$  is equal to the WACC of the investment. WACC is the cost that the owner  
408 or investor of the project must pay for the use of capital sources in order to finance the  
409 investment. A widespread practice in organizations is to use a nominal discount rate ( $d$ ) equal  
410 to the organization's WACC (Short et al., 1995). In this paper,  $d$  is assumed to be equal to  
411 WACC in order to calculate the *LCOE*.

412 The values of the *LCOE* parameters used in this study are shown in Table 4. The references  
413 that justify the choice of these parameters are also indicated in the table.

414 Table 4. Parameters used in the calculation of the *LCOE*.

Parameter	Value
$C_0$	1060-2700 USD/kWp <sup>a</sup>
$C_{clean}$	Residential: 7-11 USD/kWp/cleaning <sup>b</sup> Commercial: 4-8 USD/kWp/cleaning <sup>b</sup> Utility-scale: 0.03-0.21 USD/kWp/cleaning <sup>c</sup>
$r_d$	0.5% <sup>d</sup>
$N$	30 years <sup>e</sup>
$N_l$	20 years <sup>e</sup>
$N_d$	20 years <sup>e</sup>
$i_l$	5.3% <sup>f</sup>
$d_{ec}$	15.8% <sup>f</sup>
$rom$	4.2% <sup>f</sup>
$d$	10.9% <sup>f</sup>
$p_l$	50.0% <sup>f</sup>

415 <sup>a</sup> (Fu et al., 2018)

416 <sup>b</sup> Costs offered by PV suppliers in Aguascalientes region

417 <sup>c</sup> (Jones et al., 2016)

418 <sup>d</sup> (Branker et al., 2011; Jordan and Kurtz, 2013)

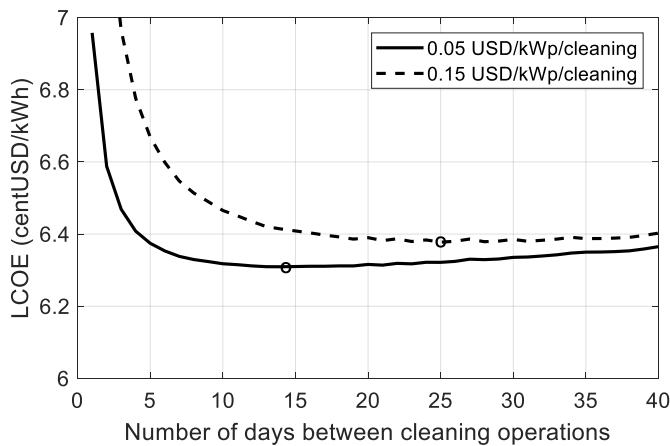
419 <sup>e</sup> (Talavera et al., 2019)

420 <sup>f</sup> (Talavera et al., 2016)

421

## 422 2.5. Optimisation method

423 A graphical optimisation method is used for every simulated scenario. It is based on plotting  
424 the *LCOE* versus the number of days between cleaning operations. The minimum of the  
425 *LCOE* function corresponds to the optimum cleaning schedule in the dry season. As an  
426 example of this graphical procedure, the *LCOE* optimisation for a 1060 USD/kWp system  
427 cost and for costs of cleaning of 0.05 and 0.15 USD/kWp is shown in Fig. 6. The circles  
428 indicate the optimal points. Cleaning intervals of 14 and 25 days are obtained respectively.  
429 It can be highlighted that the lines are quite flat near the optimal points: this suggests that  
430 multiple scenarios can be applied, with limited variation to the results.

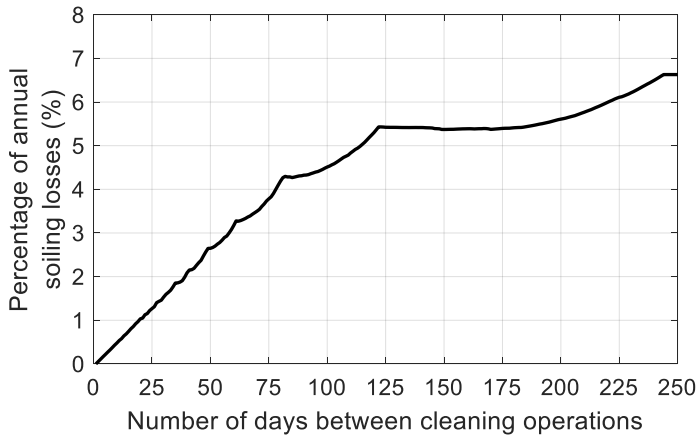


431

432 Fig. 6. Example of the graphical method to optimise cleaning schedules by minimising the  
433 *LCOE* for 1060 USD/kWp system cost. The minimum of the *LCOE* function is indicated  
434 with a circle.

## 435 3. Results

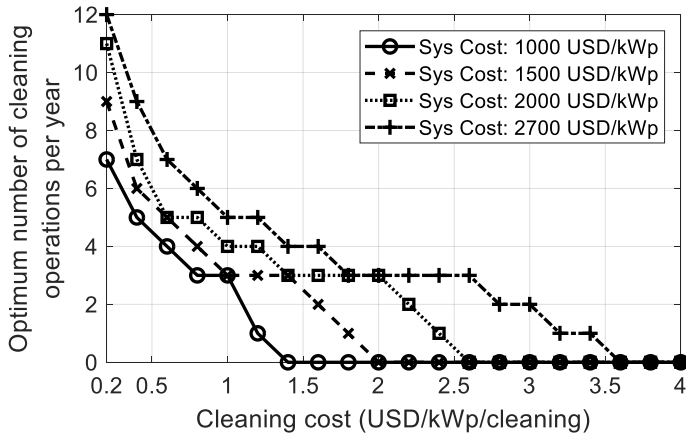
436 With the help of the energy yield model, the relation of the number of days between cleaning  
437 operations and the percentage of annual soiling losses can be characterised for  
438 Aguascalientes and is presented in Fig. 7. This graph can be useful to select a cleaning  
439 schedule that allows a specific percentage of soiling losses to be obtained. For instance, a 3%  
440 annual soiling level, which is recommended by some PV designers, can be obtained by  
441 cleaning the PV generator every 2 months in the dry season. However, these simple rules do  
442 not consider the balance between cleaning costs and benefits, and a more in deep analysis  
443 can be done with the proposed optimisation method.



444

445 Fig. 7. Relation between the number of days between cleaning operations and the percentage  
446 of annual soiling losses obtained with the energy yield model.

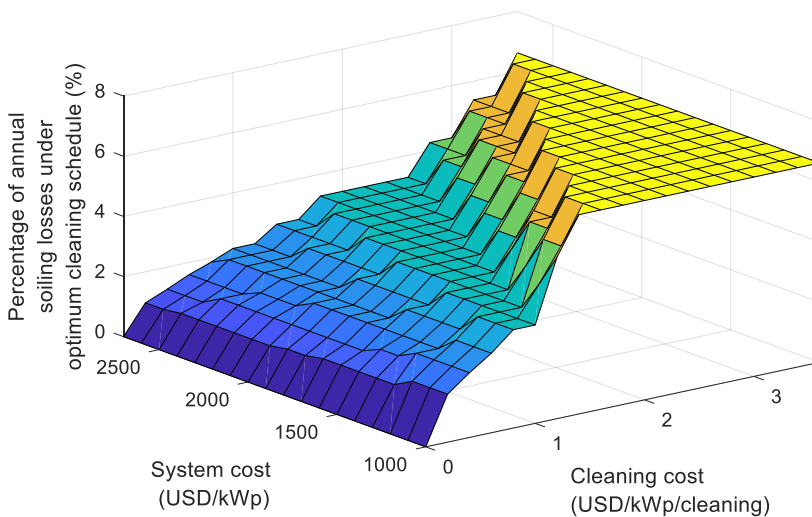
447 Optimisation results are shown in Fig. 8 for a range of cleaning costs between 0.2 and 4.0  
448 USD/kWp/cleaning and, various system investment costs from 1000 to 2700 USD/kWp. As  
449 can be seen, not only the cleaning cost determines the optimum strategy, but the system  
450 investment cost, closely related to the system size, influences as well. The influence of the  
451 system investment cost was not analysed in the existing literature. According to (Fu et al.,  
452 2018), the typical system cost nowadays in the U.S. is 1060 (utility-scale system >2MWp),  
453 1830 (commercial system between 10kWp and 2MWp) and, 2700 (residential system  
454 between 3 and 10 kWp). In Fig. 8, it can be seen that the higher the system cost, the higher  
455 the optimum number of cleaning operations per year for the same cleaning cost. This is  
456 because when the system cost increases, the weight of the operation and maintenance cost in  
457 the life cycle cost decreases. The figure also shows the threshold values of cleaning costs  
458 required for a cleaning strategy to be cost-effective. For a 1000 USD/kWp system, cleaning  
459 costs must be lower than 1.4 USD/kWp for a cleaning strategy to be useful. As the system  
460 cost increases, this threshold value also increases (2.0 USD/kWp for a 1500 USD/kWp  
461 system; 2.6 USD/kWp for a 2000 USD/kWp system; and, 3.6 USD/kWp for a 2700  
462 USD/kWp system).



463

464 Fig. 8. Optimisation of the number of cleaning operations per year as a function of the  
 465 cleaning cost and system cost for minimum *LCOE*.

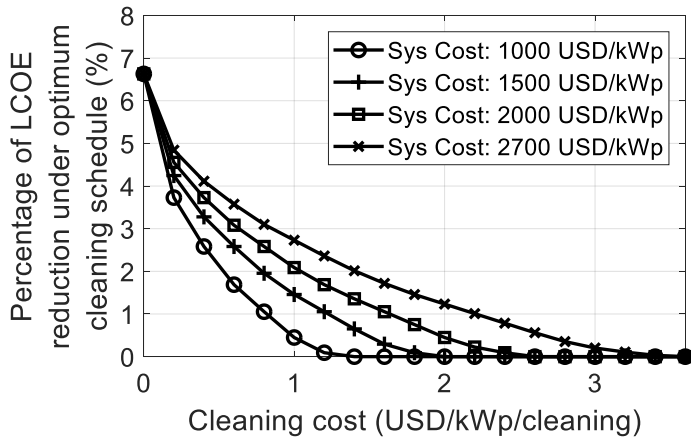
466 The optimum percentage of annual soiling losses also depends on both the cleaning cost and  
 467 the system cost, as can be seen in Fig. 9. For instance, for a cleaning cost of 1.0 USD/kWp,  
 468 the cleaning of a 1000 USD/kWp system (utility-scale) should be scheduled to assess 3.3%  
 469 annual soiling losses. However, for a 1800 USD/kWp system (commercial), the  
 470 recommendation would be to operate under 2.6% annual soiling losses and, for a 2700  
 471 USD/kWp system (residential), the recommendation would be 2.2% annual soiling losses.  
 472 These recommendations, based on minimising the *LCOE*, highlight again the influence of  
 473 the system investment cost on the optimum cleaning schedule.



474

475 Fig. 9. Percentage of annual soiling losses under optimum cleaning schedule as a function of  
476 cleaning cost and system cost.

477 The economic benefits of implementing an optimum cleaning schedule in terms of *LCOE*  
478 reduction with reference to a no cleaning strategy are investigated in Fig. 10. It can be seen  
479 that, in the ideal case in which cleaning does not represent a cost, the maximum *LCOE*  
480 reduction is 6.6%. This percentage decreases as the cleaning cost increases. The graph  
481 exhibits that the decrease in the percentage is faster for a utility-scale system than for a  
482 residential system. Therefore, utility-scale systems require lower cleaning costs for the  
483 economic benefits of cleaning to be appreciable. This verifies in real PV systems, where the  
484 cleaning costs per unit PV capacity dramatically decrease as the system size increases.



485  
486 Fig. 10. Percentage of *LCOE* reduction with reference to a no cleaning strategy as a function  
487 of cleaning cost and system cost.

488 The numerical values of the optimal cleaning strategies for typical residential, commercial  
489 and, utility-scale PV systems in Aguascalientes are shown in Table 5. Representative system  
490 costs for each system size have been taken from (Fu et al., 2018) and are indicated in the  
491 table. The cleaning costs have been set according to typical ranges offered by PV suppliers  
492 in Aguascalientes for residential and commercial systems and, according to the range  
493 proposed by (Jones et al., 2016) for utility-scale systems. As can be seen, cleaning costs can  
494 vary in a wide range depending on the cleaning method, difficulties to access the PV  
495 generator, security issues and, system size. Utility-scale systems open the possibility of using  
496 machine-assisted cleaning, which decreases considerably the cleaning cost per kWp. In Table

5, it can be seen that commercial and residential PV systems with cleaning costs from 4 to 11 USD/kWp do not need to be cleaned over the year for minimising the *LCOE*. The cost of cleaning is too high for these systems and it exceeds the threshold values analysed in Fig. 8. Such a system that operates without cleaning maintenance would generate 1674 kWh/kWp/year with an annual soiling loss level of 6.6%. Of course, these numerical results can be questioned in the real world. Most PV systems should be cleaned at least once per year in order to remove the heavy soiling that cannot be removed by the rain and that could cause mismatch or overheating problems in the PV generator or lead to cementation and permanent contamination of the surface (Toth et al., 2018). Therefore, beyond the numerical values obtained from the optimisation method, the recommendation for commercial and residential PV systems would be to clean once per year, unless the owner is not interested in cleaning. The panorama is quite different for utility-scale systems. The low cleaning costs between 0.03 and 0.21 USD/kWp allow the implementation of an optimum cleaning schedule. For the case of 0.21 USD/kWp cleaning cost, an optimum cleaning schedule each 31 days in the dry season would lower the annual soiling losses to 1.6% with a *LCOE* reduction of 3.7%. For the case of 0.03 USD/kWp cleaning cost, cleaning each 12 days in the dry season would be cost-effective, lowering the annual soiling losses to 0.6% with a *LCOE* reduction of 5.5%. Therefore, for the considered cleaning cost ranges, utility-scale systems should be cleaned between 12 and 31 days in the dry season in Aguascalientes. The use of an optimisation method such as the one proposed here results essential for the operation and maintenance scheduling in these plants.

Table 5. Numerical values of the optimisation of the cleaning schedule for residential, commercial and, utility-scale PV systems in Aguascalientes.

<b>System size</b>	Residential (3-10 kWp)	Commercial (10 kWp-2 MWp)	Utility-scale (>2 MWp)	
<b>System cost (USD/kWp)</b>	2700	1830	1060	
<b>Cleaning cost (USD/kWp/cleaning)</b>	7-11	4-8	0.21	0.03
<b>Days between cleaning operations</b>	-	-	31	12
<b>Number of cleaning operations per year</b>	0	0	7	20
<b>Annual Energy Yield (kWh/kWp)</b>	1674	1674	1764	1782

Percentage of annual soiling losses (%)	6.6	6.6	1.6	0.6
LCOE (centUSD/kWh)	16.9	11.5	6.4	6.3
Percentage of LCOE reduction (%)	0.0	0.0	3.7	5.5

520

#### 521 4. Comparative analysis

522 The different criteria proposed in the literature for optimising cleaning schedules in PV  
 523 systems were reviewed in section 1. These criteria have been implemented under the climatic  
 524 and soiling conditions of Aguascalientes in order to perform a comparative analysis for  
 525 utility-scale systems. Results of this analysis are shown in Table 6. As can be seen, for a low  
 526 cleaning cost (0.03 USD/kWp) there are very small differences in the optimum cleaning  
 527 schedule, with days between cleaning operations in the range from 10 to 12 days. For a higher  
 528 level of cleaning costs (0.21 USD/kWp), the differences are somewhat greater, ranging from  
 529 25 to 31 days between cleaning operations. It can be highlighted that the available methods  
 530 require different information to be implemented. Methods 1, 2 and, 3 require economic  
 531 revenue data, which is often subject to uncertainty, but have the advantage that are applied  
 532 only to a specific year of operation, avoiding some information needed to perform a life cycle  
 533 analysis. Method 4 is the more complex method, requiring economic revenue data, system  
 534 cost data and, the parameters for the life cycle analysis. Our proposed method does not  
 535 require economic revenue data, but require system cost data and the parameters for the life  
 536 cycle analysis. Therefore, taking into account that the differences in the optimisation results  
 537 are small for the available methods in utility-scale systems, it can be concluded that any  
 538 method could be used with reliability. The choice of a specific method would depend on the  
 539 availability of information such as economic revenue data, system cost data and, parameters  
 540 for calculating the economics of the life cycle.

541 Table 6. Comparative analysis under the climatic and soiling conditions of Aguascalientes of  
 542 the existing criteria for optimising cleaning schedules in utility-scale PV systems.

Method ID	Reference	Criterion	Days between cleaning operations (0.21 USD/kWp/cleaning)	Days between cleaning operations (0.03 USD/kWp/cleaning)
-----------	-----------	-----------	--	--



1	(Tanesab et al., 2018) <sup>a</sup>	Annual revenue loss due to soiling equals annual cleaning cost	28	11
2	(Besson et al., 2017) <sup>a</sup>	Maximise annual revenue minus annual cleaning cost	31	10
3	(Jones et al., 2016) <sup>a</sup>	Minimise {(annual revenue loss due to soiling plus annual cleaning cost)/(annual revenue)}	25	10
4	(You et al., 2018) <sup>a, b, c</sup>	Maximise net present value	25	10
5	This study <sup>c</sup>	Minimise levelised cost of energy	31	12

543 <sup>a</sup> Revenue per generated kWh=7 centUSD

544 <sup>b</sup> Annual escalation rate of revenue per generated kWh=2.5%

545 <sup>c</sup> System cost=1000 USD/kWp

546

## 547 **5. Conclusions**

548 A novel method for optimising the cleaning schedule in photovoltaic systems based on  
 549 minimising the levelised cost of energy has been developed. The method takes into account  
 550 the life cycle costs, allowing the influence of the system investment cost on the optimum  
 551 cleaning schedule to be analysed, and does not depend on economic revenue data, which is  
 552 often subject to uncertainty. The method has been applied to Aguascalientes, central Mexico,  
 553 where an experimental characterisation of natural soiling on optimally tilted crystalline  
 554 silicon modules was performed. The experimental soiling measurements exhibited a soiling  
 555 rate of -0.16% in the dry season and a stabilization of the soiling losses at 11.2% after 70  
 556 days of exposure. The method has been also compared to other existing criteria for optimising  
 557 cleaning schedules.

558 The main conclusions of the study are:

559 - While the cleaning costs play an important role for optimising cleaning schedules, the  
 560 system investment costs also influence as a second factor. The influence of these investment  
 561 costs only can be analysed with an optimisation method that considers the whole life cycle  
 562 of the system, such as the one proposed in this paper.

563 - Residential and commercial systems minimise the levelised cost of energy without carrying  
 564 out cleaning operations in Aguascalientes. One cleaning per year would make possible to

565 remove heavy soiling, and avoid permanent damage and contamination to the modules. More  
566 cleaning operations are not recommended because of the high cleaning costs.

567 - Utility-scale systems should be cleaned in intervals between 12 and 31 days in  
568 Aguascalientes as a function of the cleaning costs (between 0.03 and 0.21 USD/kWp in this  
569 study).

570 - The comparative analysis under the conditions of Aguascalientes to other existing criteria  
571 to optimise cleaning schedules for utility-scale systems revealed that every method gives  
572 similar results, with a maximum difference of 6 days in the cleaning schedule. However, the  
573 methods require different information to be implemented and, therefore, the choice of a  
574 suitable method depends on the data available in each specific project.

575 The methodology proposed in this paper could be adapted to other locations with different  
576 climatic, soiling and, economic conditions. However, in the current study, some  
577 simplifications in the energy yield calculation have been considered because of the  
578 peculiarities of the typical conditions in Aguascalientes, where the dry and wet seasons are  
579 clearly differentiated, the dry season has very scarce rainfall and, the wet season has frequent  
580 storms typically every day. Other climates would require a more in deep analysis of the  
581 soiling rate seasonal variability and advanced rainfall forecasting techniques.

## 582 **Acknowledgments**

583 Pedro M. Rodrigo and Sebastián Gutiérrez acknowledge the Science and Technology  
584 National Council of México (CONACYT) for the economic support as members of the  
585 National System of Researchers. Eduardo F. Fernández is supported by the Spanish  
586 “Ministerio de Ciencia, Innovación y Universidades (MICINN)” under the Ramón y Cajal  
587 2017 program. Part of this work was funded by the “Fondo Fomento a la Investigación”  
588 program of Panamericana University under the project UP-CI-2017-ING-AGS-01. Part of  
589 this work was also funded through the European Union's Horizon 2020 research and  
590 innovation programme under the NoSoilPV project (Marie Skłodowska-Curie grant  
591 agreement No. 793120).

592 The authors thank the Coordinación General del Servicio Meteorológico Nacional (CGSMN)  
593 of the Comisión Nacional del Agua (CONAGUA) of Mexico because of the supply of the

594 meteorological data used in this research. The authors also thank Jerónimo Álvarez and  
595 Arturo Acero because of the operation and maintenance of the experimental set-up.

## 596 **References**

- 597 Besson, P., Munoz, C., Ramirez-Sagner, G., Salgado, M., Escobar, R., Platzer, W., 2017.  
598 Long-Term Soiling Analysis for Three Photovoltaic Technologies in Santiago Region.  
599 *IEEE J. Photovoltaics* 7, 1755–1760.
- 600 Branker, K., Pathak, M.J.M., Pearce, J.M., 2011. A review of solar photovoltaic levelized  
601 cost of electricity. *Renew. Sustain. Energy Rev.* 15, 4470–4482.
- 602 Cabanillas, R.E., Munguía, H., 2011. Dust accumulation effect on efficiency of Si  
603 photovoltaic modules. *J. Renew. Sustain. Energy* 3.
- 604 Centro nacional de Control de Energía (CENACE), 2018. Subastas de largo plazo [WWW  
605 Document]. URL  
606 <https://www.cenace.gob.mx/Paginas/Publicas/MercadoOperacion/SubastasLP.aspx>  
607 (accessed 8.22.19).
- 608 Coello, M., Boyle, L., 2019. Simple Model for Predicting Time Series Soiling of  
609 Photovoltaic Panels. *IEEE J. Photovoltaics* 9, 1382–1387.
- 610 Conceição, R., Silva, H.G., Fialho, L., Lopes, F.M., Collares-Pereira, M., 2019. PV system  
611 design with the effect of soiling on the optimum tilt angle. *Renew. Energy* 133, 787–  
612 796.
- 613 Costa, S.C.S., Diniz, A.S.A.C., Kazmerski, L.L., 2018. Solar energy dust and soiling R&D  
614 progress: Literature review update for 2016. *Renew. Sustain. Energy Rev.* 82, 2504–  
615 2536.
- 616 Costa, S.C.S., Diniz, A.S.A.C., Kazmerski, L.L., 2016. Dust and soiling issues and impacts  
617 relating to solar energy systems: Literature review update for 2012-2015. *Renew.*  
618 *Sustain. Energy Rev.* 63, 33–61.
- 619 Fathi, M., Abderrezek, M., Grana, P., 2017. Technical and economic assessment of  
620 cleaning protocol for photovoltaic power plants: Case of Algerian Sahara sites. *Sol.*

- 621 Energy 147, 358–367.
- 622 Fu, R., Feldman, D., Margolis, R., 2018. U . S . Solar Photovoltaic System Cost  
623 Benchmark : Q1 2018. NREL 1–47.
- 624 Fuentealba, E., Ferrada, P., Araya, F., Marzo, A., Parrado, C., Portillo, C., 2015.  
625 Photovoltaic performance and LCoE comparison at the coastal zone of the Atacama  
626 Desert, Chile. *Energy Convers. Manag.* 95, 181–186.
- 627 Gostein, M., Caron, J.R., Littmann, B., 2014. Measuring soiling losses at utility-scale PV  
628 power plants, in: 2014 IEEE 40th Photovoltaic Specialist Conference, PVSC 2014. pp.  
629 885–890.
- 630 Gostein, M., Littmann, B., Caron, J.R., Dunn, L., 2013. Comparing PV power plant soiling  
631 measurements extracted from PV module irradiance and power measurements, in:  
632 Conference Record of the IEEE Photovoltaic Specialists Conference. pp. 3004–3009.
- 633 Hay, J.E., 1979. Calculation of monthly mean solar radiation for horizontal and inclined  
634 surfaces. *Sol. Energy* 23, 301–307.
- 635 Instituto Nacional de Ecología y Cambio Climático (INECC), 2019. Sistema Nacional de  
636 Información de la Calidad del Aire (SINAICA) [WWW Document]. URL  
637 <https://sinaica.inecc.gob.mx/> (accessed 8.23.19).
- 638 International Electrotechnical Commission, 2017. IEC 61724-1: Photovoltaic system  
639 performance – Part 1: Monitoring. Geneva, Switzerland.
- 640 International Electrotechnical Commission (IEC), 2011. IEC 61853–1: Photovoltaic (PV)  
641 Module Performance Testing and Energy Rating - Part 1: Irradiance and Temperature  
642 Performance Measurements and Power Rating. Geneva, Switzerland.
- 643 Iqbal, M., 1983. An introduction to solar radiation. Academic Press, Toronto.
- 644 Jiang, Y., Lu, L., Lu, H., 2016. A novel model to estimate the cleaning frequency for dirty  
645 solar photovoltaic (PV) modules in desert environment. *Sol. Energy* 140, 236–240.
- 646 Jones, R.K., Baras, A., Saeri, A.A., Al Qahtani, A., Al Amoudi, A.O., Al Shaya, Y.,  
647 Alodan, M., Al-Hsaien, S.A., 2016. Optimized Cleaning Cost and Schedule Based on

- 648 Observed Soiling Conditions for Photovoltaic Plants in Central Saudi Arabia. *IEEE J.*  
649 *Photovoltaics* 6, 730–738.
- 650 Jordan, D.C., Kurtz, S.R., 2013. Photovoltaic degradation rates - An Analytical Review.  
651 *Prog. Photovoltaics Res. Appl.* 21, 12–29.
- 652 Kalogirou, S.A., Agathokleous, R., Panayiotou, G., 2013. On-site PV characterization and  
653 the effect of soiling on their performance. *Energy* 51, 439–446.
- 654 Kimber, A., Mitchell, L., Nogradi, S., Wenger, H., 2007. The effect of soiling on large grid-  
655 connected photovoltaic systems in California and the Southwest Region of the United  
656 States, in: *Conference Record of the 2006 IEEE 4th World Conference on*  
657 *Photovoltaic Energy Conversion, WCPEC-4.* pp. 2391–2395.
- 658 Luque, E.G., Antonanzas-Torres, F., Escobar, R., 2018. Effect of soiling in bifacial PV  
659 modules and cleaning schedule optimization. *Energy Convers. Manag.* 174, 615–625.
- 660 Micheli, L., Fernández, E.F., Muller, M., Almonacid, F., 2019. Extracting and Generating  
661 PV Soiling Profiles for Analysis, Forecasting and Cleaning Optimization (under  
662 review). *IEEE J. Photovoltaics*.
- 663 Micheli, L., Ruth, D., Muller, M., 2017. Seasonal Trends of Soiling on Photovoltaic  
664 Systems, in: *2017 IEEE 44th Photovoltaic Specialist Conference (PVSC).* IEEE, pp.  
665 2301–2306. <https://doi.org/10.1109/PVSC.2017.8366381>
- 666 Pérez-Higueras, P.J., Almonacid, F.M., Rodrigo, P.M., Fernández, E.F., 2018. Optimum  
667 sizing of the inverter for maximizing the energy yield in state-of-the-art high-  
668 concentrator photovoltaic systems. *Sol. Energy* 171, 728–739.
- 669 Rodrigo, P.M., 2017. Improving the profitability of grid-connected photovoltaic systems by  
670 sizing optimization, in: *2017 IEEE Mexican Humanitarian Technology Conference,*  
671 *MHTC 2017.* pp. 1–6.
- 672 Rodrigo, P.M., Velázquez, R., Fernández, E.F., 2016. DC/AC conversion efficiency of  
673 grid-connected photovoltaic inverters in central Mexico. *Sol. Energy* 139, 650–665.
- 674 Rus-Casas, C., Aguilar, J.D., Rodrigo, P., Almonacid, F., Pérez-Higueras, P.J., 2014.

- 675 Classification of methods for annual energy harvesting calculations of photovoltaic  
676 generators. *Energy Convers. Manag.* 78, 527–536.
- 677 Sánchez-Carbajal, S., Rodrigo, P.M., 2019. Optimum Array Spacing in Grid-Connected  
678 Photovoltaic Systems considering Technical and Economic Factors. *Int. J.*  
679 *Photoenergy* 2019.
- 680 Servicio Meteorológico Nacional, 2019. Normales climatológicas por estado [WWW  
681 Document]. URL [https://smn.cna.gob.mx/es/climatologia/informacion-](https://smn.cna.gob.mx/es/climatologia/informacion-climatologica/normales-climatologicas-por-estado)  
682 [climatologica/normales-climatologicas-por-estado](https://smn.cna.gob.mx/es/climatologia/informacion-climatologica/normales-climatologicas-por-estado) (accessed 8.23.19).
- 683 Short, W., Packey, D.J., Holt, T., 1995. A manual for the economic evaluation of energy  
684 efficiency and renewable energy technologies. *Natl. Renew. Energy Lab. NREL/TP-*  
685 *462-5173*.
- 686 Sulaiman, S.A., Razif, M.R.M., Han, T.D., At Naw, S.M., Tamili, S.N.A., 2018. Impact of  
687 Soiling Rate on Solar Photovoltaic Panel in Malaysia, in: *MATEC Web of*  
688 *Conferences*.
- 689 Talavera, D.L., Ferrer-Rodríguez, J.P., Pérez-Higueras, P., Terrados, J., Fernández, E.F.,  
690 2016. A worldwide assessment of levelised cost of electricity of HCPV systems.  
691 *Energy Convers. Manag.* 127, 679–692.
- 692 Talavera, D.L., Muñoz-Cerón, E., Ferrer-Rodríguez, J.P., Pérez-Higueras, P.J., 2019.  
693 Assessment of cost-competitiveness and profitability of fixed and tracking  
694 photovoltaic systems: The case of five specific sites. *Renew. Energy* 134, 902–913.
- 695 Tanesab, J., Parlevliet, D., Whale, J., Urmee, T., 2018. Energy and economic losses caused  
696 by dust on residential photovoltaic (PV) systems deployed in different climate areas.  
697 *Renew. Energy* 120, 401–412.
- 698 Toth, S., Muller, M., Miller, D.C., Moutinho, H., To, B., Micheli, L., Linger, J., Engrakul,  
699 C., Einhorn, A., Simpson, L., 2018. Soiling and cleaning: Initial observations from 5-  
700 year photovoltaic glass coating durability study. *Sol. Energy Mater. Sol. Cells* 185,  
701 375–384.
- 702 Urrejola, E., Antonanzas, J., Ayala, P., Salgado, M., Ramírez-Sagner, G., Cortés, C., Pino,

**Preprint:** Rodrigo PM, Gutierrez S, Micheli L, Fernández EF, Almonacid F. Optimum cleaning schedule of photovoltaic systems based on levelised cost of energy and case study in central Mexico. Sol Energy 2020;209:11–20.

DOI: [10.1016/j.solener.2020.08.074](https://doi.org/10.1016/j.solener.2020.08.074)

703 A., Escobar, R., 2016. Effect of soiling and sunlight exposure on the performance ratio  
704 of photovoltaic technologies in Santiago, Chile. Energy Convers. Manag. 114, 338–  
705 347.

706 You, S., Lim, Y.J., Dai, Y., Wang, C.-H., 2018. On the temporal modelling of solar  
707 photovoltaic soiling: Energy and economic impacts in seven cities. Appl. Energy 228,  
708 1136–1146.

709